Heliyon 10 (2024) e24041

Contents lists available at ScienceDirect

Heliyon

journal homepage: www.cell.com/heliyon

Research article

Design, construction and evaluation of a miniature soil bin plus predicting the measured parameters during primary tests using ANFIS

Arash Lajani [a], Ali Mohammad Nikbakht [a], Mohammad Askari [b,*], Mahmood Reza Salar [c]

[a] Department of Biosystem Engineering, Faculty of Agriculture, Urmia University, Urmia, Iran
[b] Department of Biosystem Engineering, Faculty of Agricultural Engineering, Sari Agricultural Sciences and Natural Resources University, Sari, Iran
[c] Department of Biosystem Engineering, Faculty of Agriculture, Shiraz University, Shiraz, Iran

ARTICLE INFO

Keywords:
ANFIS
Inceptisols
Soil bin
Soil-tool interaction
Soil movement
Tillage

ABSTRACT

A clear understanding of soil-machine interaction is utilised in many areas, such as rational design and performance optimisation of soil-engaging tools/implements. This research developed a new soil bin to investigate the interaction between soil-narrow tines and soil failure. The new soil bin consisted of a chassis, a bin, a variable speed carriage and a bolt and nut type power transmission system between the motor and carriage. The design criteria of the new soil bin were based on the drive system's immediate acceleration of the carriage unit. A curved chisel tine was tested to evaluate the system's capabilities. Three parameters, including lift height, failure side area and forward failure distance, were investigated at two forward speeds of 0.037 and 0.05 m/s and three rake angles of 5°, 10° and 20°. An analysis of variance (ANOVA) test revealed the effect of rake angle on the lift height, failure side area, and forward failure distance was significant ($P < 0.01$). However, the forward speed did not have any significant influence on parameters. Also, the lift height and failure side area increased significantly ($P < 0.01$) by increasing the rake angle, while the forward failure distance decreased. Regarding soil failure, the results were in harmony with Godwin and Spoor's model. The regression and ANFIS models were developed to predict the output parameters by considering input parameters. The R^2 values and ANFIS models were 0.4895, 0.7264, 0.9856, and 0.9999, 1, 1, respectively, for lift height, side area, and forward distance. Therefore, ANFIS approach was more accurate for predicting soil failure parameters.

1. Introduction

For a long time, soil-engaging tools have been designed trial-and-error, as the soil-tool interactions involved have not been defined yet. According to Ref. [1]. Soil disturbance and forces developed at the soil interface and the tool are two important aspects of soil–tool interaction. Soil–tool interaction involves two aspects: on the one hand are the forces developed at the interface of the soil and the tool, such as draught, side and vertical forces; on the other hand is the displacement of soil particles, also known as soil disturbance [2,3]. Classical soil failure theories have for quite some time relied on the various trials aimed at predicting tillage forces under different

* Corresponding author.
E-mail address: m.askari@sanru.ac.ir (M. Askari).

https://doi.org/10.1016/j.heliyon.2024.e24041
Received 25 May 2023; Received in revised form 24 December 2023; Accepted 2 January 2024
Available online 3 January 2024

Symbols and abbreviation description

ANOVA	Analysis of variance
ANFIS	Adaptive neuro-fuzzy inference system
ANN	Artificial neural network
FIS	Fuzzy inference system
MSE	Mean square error
P_{max}	required maximum power(kW)
V	travel speed of the carriage(m/s)
P_{line}	line pull (kN)
η	transmission system efficiency
S	Speed
A	Rake angle
CRD	complete randomised design
DC	direct current
MFs	Member functions

conditions [4–10]. Critical state soil failure theories and passive soil pressure have commonly been used in such cases [11]. The soil failure mode is determined by tine speed, geometry, density, and soil moisture content [9]. There has been a growing interest regarding the suitability of the existing theories in solving different problems, such as the changes in soils and tools; thus, more research is still to be conducted to clearly understand the soil failure mechanics under the impact of tillage tools. Conservation tillage has largely replaced conventional tillage in the United States, South America, Africa, and Asia and is becoming more popular in Europe [12]. Minimum soil disturbance using narrow tines is of principal importance in conservation tillage. On the other hand, soil break up is an important factor in plant growth [13]. A fine clod structure and slight compaction are desirable for proper contact between soil and seed.

Studies are still being conducted concerning narrow tools designed to reach the optimised case. Narrow tools used in conservation tillage include chisel ploughs, discs and harrows, most of which have curved tines. However, the interaction between soil and curved tine has not been sufficiently studied. Further, most analytical models of soil failure geometric patterns were based on simplified flat blade, neglecting standard tine shapes such as curved or winged tines [14]. On the other hand, most field studies on tillage tools have been limited by the variable and unpredictable soil nature [15]. This problem has been overcome primarily by using experimental soil bins where soil-tool interactions can be evaluated in controlled laboratory conditions in a soil bin [16]. Different types or aspects of soil bin facilities have been developed with varying levels of instrumentation [17–19]. The best kind of soil bin to observe the soil failure with tines is a glass-sided one. Many researchers have employed this soil bin to observe the failure patterns [4,9,11,20–22].

The main problem of these soil bins was their large dimension (outdoor) that was not suitable for test of narrow tines, use of no grit on the glassy walls to prevent slippage and low profile. Accordingly, a small soil bin test facility was developed in the present study to investigate the interaction between soil and narrow tines (plane or curved) with gritty glassy walls and a high profile to observe the failure pattern better.

Currently, prediction methods are welcome for curtailing the time and cost-consuming field operation. They are divided into three groups involving computer, mathematics and regression models. Computer models are the newest ones and highly accurate relative to others. One of the computer model approaches is a combination of artificial neural network (ANN) and fuzzy inference system (FIS) named adaptive neuro-fuzzy inference system (ANFIS) with the benefits of both approaches. On the other hand, because of stochastic and non-linear features of soil-tool interactions, ANFIS is the best choice as an artificial intelligence approach. Very few researches were done on applying ANFIS to predict related parameters to soil-tool interaction [23–25] in farm situation and no research was done at soil bin situation. Therefore, the first aim of this work was to introduce the design criteria, considerations and description of the mechanical and electrical components of the new indoor facility and its evaluation through conducting the tests. Secondly, the results of the tests and the effects of forward speed and rake angle on soil failure parameters would be reported. Moreover, the regression and ANFIS models of studied parameters related to soil failure (lift height, failure side area and forward failure distance) will be developed and correlation coefficient (R^2) plus mean square error (MSE) between predicted and obtained data will be reported.

2. Materials and methods

2.1. System design

The design criteria of the new facility were as follows: A) Drive system should immediately accelerate tool carriage because the soil bin is small, portable and short. B) The carriage must run forwards and backwards to conduct a 2-way tillage operation. C) The employed narrow tines (with sizes of up to 4 cm wide) must not have any boundary interaction with the bin walls. D) The brake system has to be efficient for safety. E) The process of loading and unloading the soil must be simple. F) The operating speed, rake angle, soil moisture content, compaction, and other essential parameters must be measured and controlled. G) The mode of soil failure must be observed.

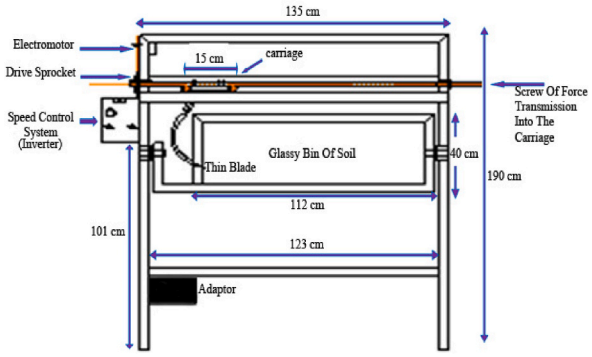

Fig. 1. The schematic of the new test facility.

Fig. 2. Rotation of the bin in the stage of soil preparation.

Fig. 3. Position of the bin in the tests.

The required soil bin was designed based on the above criteria (A to G). The new system consisted of a chassis, a bin, a variable speed carriage plus a bolt and nut type power transmission system between the motor and carriage. The setup was designed by AutoCAD 2009 package and then fabricated. Fig. 1 shows the schematic of the soil bin.

2.2. Bin

The bin (112 cm long, 30 cm wide and 40 cm deep) was installed on the chassis using two shafts, an arrangement that allowed the operator to rotate the bin to facilitate its loading and unloading (Fig. 2). For observing the soil failure, both sides of the bin were blocked by the glass. The walls were covered with grit to prevent any slipping. One of the vertical sides of the soil face was marked with a chalk dust grid (30 mm squares) to determine the soil movement. The bin was rotated and fixed during the test (Fig. 3).

As shown in Fig. 4, a method developed by Ref. [26] was used to determine the bin width. Tillage depth and soil bin inner width were 13 and 30 cm, respectively, with a free space between the cutting edge and the bin wall for a 5 cm wide blade. The minimum bin

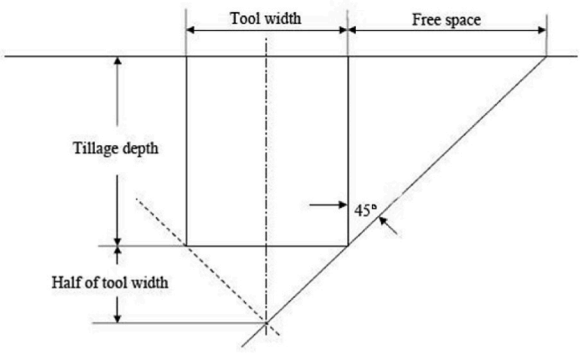

Fig. 4. Estimation of bin depth and width.

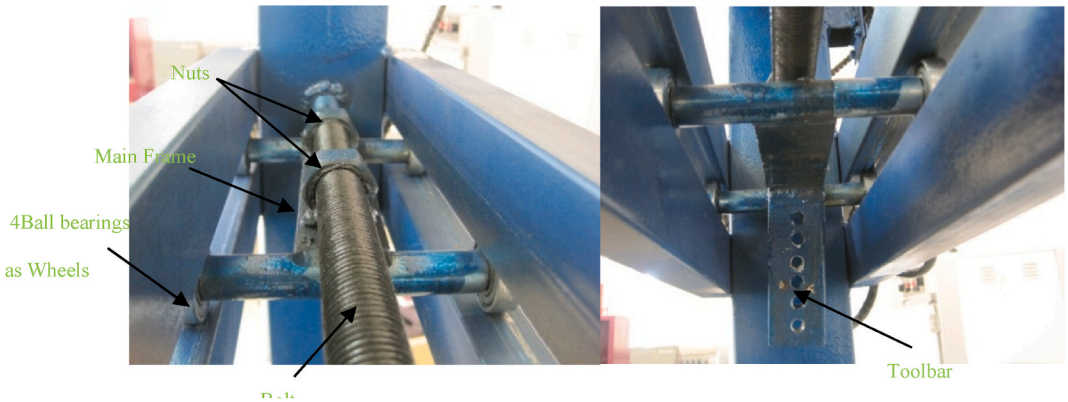

Fig. 5. The main frame and toolbar of the carriage.

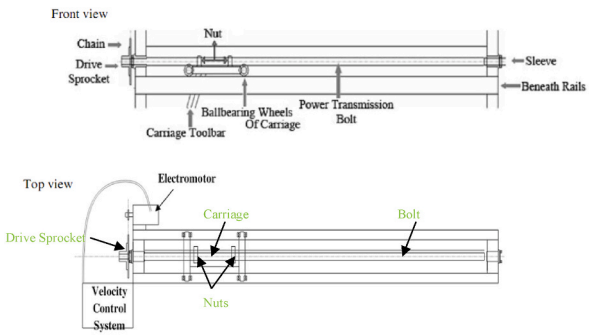

Fig. 6. The carriage and drive system.

depth was equal to tillage depth plus half the width of a tool to eliminate the boundary effect (Fig. 4). A 5 cm wide tool requires a depth of 12.5 cm, while the tillage depth was 10 cm.

2.3. Carriage unit

The carriage unit was supported by four rails. This unit supported the tine and consisted of the main frame, four ball bearings used as wheels and a holed toolbar to mount the tine (Fig. 5). An electromotor moved the carriage along the rails. Fig. 6 indicates the general arrangement of the carriage and drive system. Two micro switches were provided at the two ends of the bin to stop the carriage.

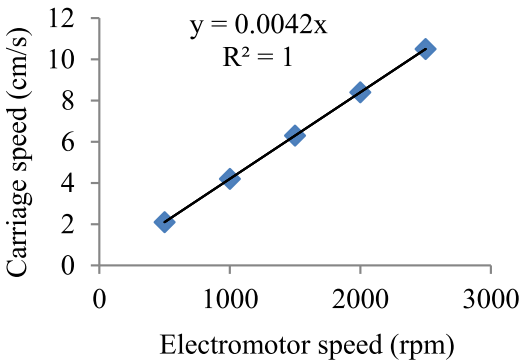

Fig. 7. Calibration curve of the carriage speed.

Table 1
Measured properties of soil.

Moisture content (db) (%)	Porosity (%)	Void Ratio	Bulk density (g/cm^3)	Degree of saturation	Organic Carbon (g/100g)	pH
12.1	0.52	1.08	1.5	0.205	0.74	7.8

2.4. Drive system

An electric motor was used to move the carriage by a bolt and nut type power transmission system. The power range can be calculated using the highest values anticipated for line pull and line speed as follows:

$$P_{max} = \frac{VP_{line}}{\eta} \quad (1)$$

Where P_{max} = required maximum power (kW), V = line speed or travel speed of the carriage (m/s), P_{line} = line pull (kN), η = transmission system efficiency.

The line pull includes draft, rolling resistance of ball bearings and acceleration resistance. The draft of a standard chisel tine (4 cm wide) was estimated by Ref. [27]. The motor was then chosen, and the sufficient transmission ratio was determined based on the carriage's speed requirement (maximum 0.1 m/s) with the power range equal to or larger than the power range. Finally, a DC (direct current) electromotor of 0.275 kW (24 V, 11.5 A, 2500 rpm) was selected for the system.

2.5. Power transmission system

The electromotor drove the sprocket through a chain-sprocket link. A long bolt was fixed on the drive sprocket. The power was transmitted to the bolt and into the carriage unit using a bolt-nut system (Figs. 5 and 6). An inverter controlled the operation of the electromotor and carriage unit (Fig. 1). The inverter was able to set the carriage to any desired speed from 0.01 to 0.1 m/s and to move the carriage forwards and backwards. The recorded data of electromotor output speed was plotted against carriage speed to form the calibration curve, as shown in Fig. 7. As can be seen, the calibration curve indicates a high degree of linearity.

2.6. Soil fitting equipment

Before the test, a developed wooden rule limited the bin area to prevent soil strewing during the soil preparation stage (Fig. 2). After pouring soil into the bin, the soil surface was levelled with a hand leveller to ensure there was an even distribution of the soil. The loose soil was compacted to the required density by a small roller. In the study, this action was continued on all layers until the bin was filled. After marking the soil, the glassy wall was placed and the bin was rotated and fixed until ready to start the test. To increase the soil moisture content, water was sprayed on the soil layers using a sprinkler.

2.7. Preliminary tests

The preliminary tests were conducted using a curved chisel tine with a 4 cm width at a constant depth of 12 cm, two speeds of 0.037 and 0.05 m/s (the speeds selection was under the effect of ratio of drive and driven gears plus converter limitations) and three rake angles of 5, 10 and 20° in clay loam soil (43 % clay, 35 % sand and 22 % silt) with the 4 replications. Soil class was inceptisols and its moisture and other physical properties were measured over 5 points of the bin prior to each test, detailed in Table 1. With the two

Fig. 8. Gridding the soil surface by gypsum.

speeds (S), three rake angles (A) and four replications for each run, 24 trials were conducted based on a complete randomised design (CRD). In each run, the lift height, failure side area and forward failure distance were measured. It was assumed that mentioned parameters are independent of each other but at least one of them is dependent on others. The images were recorded throughout the runs using a camera to evaluate soil failure visually.

2.8. Gridding the soil surface

After the soil channel was completely filled, gridding (to create 3 × 3 cm square houses) of the soil was considered in order to observe how the soil breaks in each lane. For this purpose, a plate of wood with parallel grooves spaced 3 cm apart was used. The wooden piece was placed on the surface of the soil, then by filling gypsum, the grooves that the distance of each of they were 3 cm apart and were created on the surface of the soil (Fig. 8).

2.9. Soil failure theories

There are many soil failure theories such as those developed by Refs. [4,7,8,10,28,29] where the tool shape and soil are, more often than not, considered for the operating condition. However, the effect of forward speed is ignored in all such models. In this research, the static models of soil failure were considered due to the very low speed of tine. As the tillage tool speed increases, dynamic effects on cutting force become more considerable [30]. As [7] reported, the experimental verification of the narrow tine theories was limited to tines whose working depth/width ratios, termed aspect ratios, were approximately 6 or less. They identified two soil failure mechanisms: an upper failure zone above the critical depth where the soil was displaced forward, sideways, and upward (crescent failure), and a lower failure zone where the displaced soil had only forward and sideways (lateral failure). The two main parameters defined when soil failure occurs by tine are lift height and forward failure distance. As tine moves forward, the soil ahead of the tine rises to the point where shear occurs. The amount of upward soil movement is defined as the lift height. The distance ahead of the tine at which the distinct shear plane breaks the surface is called the forward failure distance. Another parameter defined in this work was the failure side area, which is the side area of soil disturbance observed through the glass wall.

2.10. Data analysis and prediction

Soil failure parameters, including lift height, failure side area and forward failure distance, were analysed as a function of tine speed and its rake angle. Analysis of obtained data was conducted using SPSS16 statistical software. Moreover, disturbed profiles were analysed by visual and statistical interpretation. Additionally, the linear regression modelling was done using $SPSS_{16.0}$ software and the results were compared with the results of ANFIS part at MATLAB software.

2.11. Adaptive neuro-fuzzy inference system (ANFIS)

If the input data are dusky or subject to a relatively high uncertainty, a fuzzy system such as ANFIS will be a better choice (Pentos and Pieczarka, 2017). The membership functions (MFs) are changed during the learning process at ANFIS and the adaptation of them is conducted through a gradient vector. The gradient vector provides an evaluation measure for the assessments of ANFIS modeling performance.

There were a total of 24 data points available for input variables (rake angle and speed of tine) and output variables (lift height, side area and forward distance). Many ANFIS models with various MFs could be developed to find the best ANFIS model for predicting the outputs. Data were split into 18 data for training and 6 data for testing portions to avoid the over fitting drawback. Mean square error (MSE) and determination coefficient (R^2) were considered to evaluate the ANFIS models that are shown in Table 5 as described below,

Table 2
Mean data obtained from the preliminary tests.

Treatments	Speed (m/s)	Rake angle (degree)	Lift height (cm)	Failure side area (cm2)	Forward failure distance (cm)
1	0.05	5	2.75	117.90	27.24
2	0.037	5	2.11	116.34	26.81
3	0.05	10	4.37	153.55	24.59
4	0.037	10	4.12	153.03	23.75
5	0.05	20	4.96	154.32	22.72
6	0.037	20	3.84	153.90	21.68

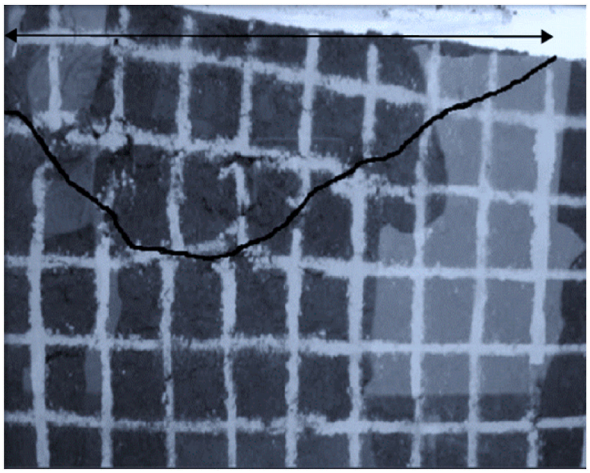

Fig. 9. Forward failure distance and failure side area in the first repetition of treatment 1.

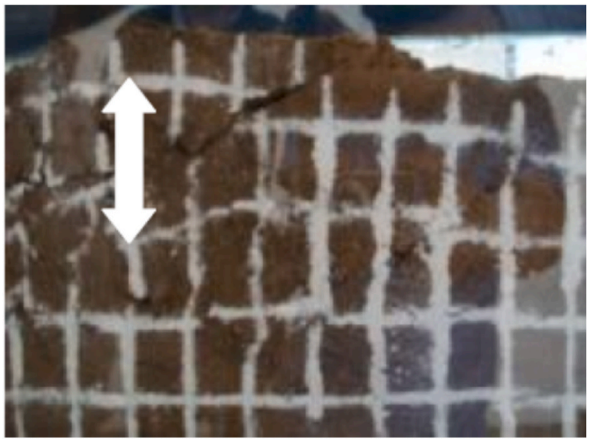

Fig. 10. Lift height in the first repetition of case 1.

respectively.

$$MSE = \frac{1}{n}\sum_{i=1}^{n}(Ypr\text{-}Yac)^2 \tag{1a}$$

$$R^2 = \frac{\sum_{i=1}^{n}(Ypr\text{-}Yac)^2}{\sum_{i=1}^{n}(Ypr\text{-}Yme)^2} \tag{2}$$

Where Yac, Ypr and Yme are measured, predicted and mean values of the developed models, respectively.

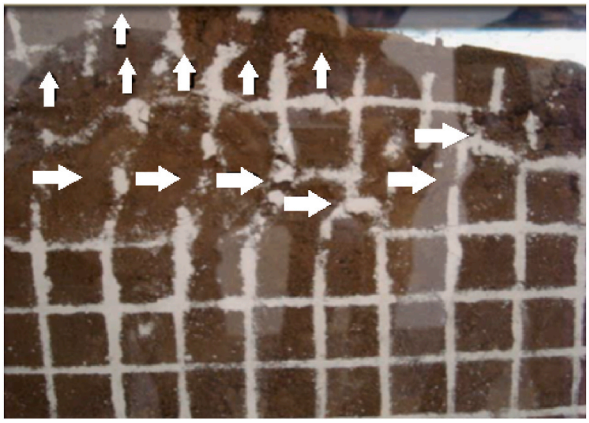

Fig. 11. Soil failure pattern in all tests.

Table 3
Analysis of variance (ANOVA) of forward speed and rake angle effects on the studied parameters.

Source of variation	Degree of freedom	Mean square		
		Lift height	Failure side area	Forward failure distance
Speed (S)	1	2.7 ^{ns}	4.118 ^{ns}	3.468 ^{ns}
Rake angle (A)	2	9.608**	3570.381**	47.181**
S × A	2	0.384 ^{ns}	0.783 ^{ns}	0.189 ^{ns}
Error	18	1.058	62.114	2.957
Total	24			

ns Not significant.
**P < 0.01.

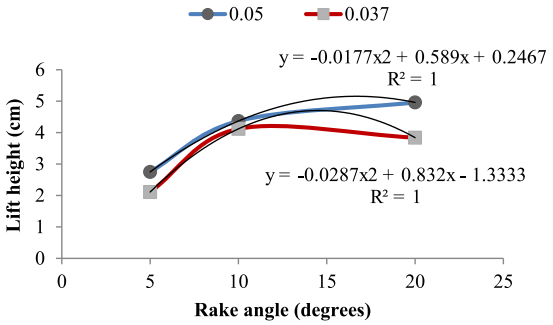

Fig. 12. The relationship between lift height and rake angle.

3. Results and discussion

3.1. Preliminary tests

Table 2 summarises the values of the measured parameters. The presented values were smoothed using four running averages. Forward failure distance and failure side area, lift height in first the repetition of treatment 1 and soil failure pattern of all tests are shown in Figs. 9–11, respectively. The aspect ratio of the tested tine was (d/w = 3). White arrows in Fig. 11 show that the soil displaced forward, sideway and upward components and the same thing occurred in researches conducted by Refs. [7,31]. This picture shows that the working depth has not yet reached the critical depth. Because below the critical depth, the soil only goes to the sides and does not rise. Moreover, as was anticipated from the tine aspect ratio, crescent failure occurred in the tests. Many researchers, such as [32] reported that soil disturbance significantly increased with the increase in the working depth, but not with the working speed, as the effects of the latter on soil disturbance were not detected. It should also be noted that there are similar trends between the results of this research and the previous researches.

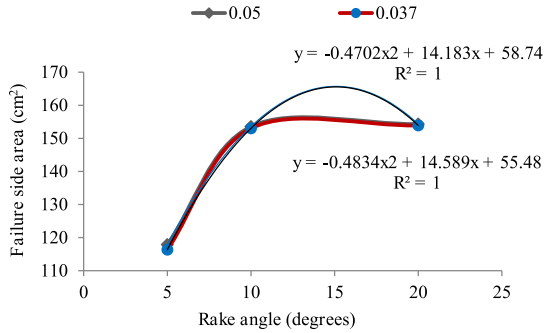

Fig. 13. The relationship between failure side area and rake angle.

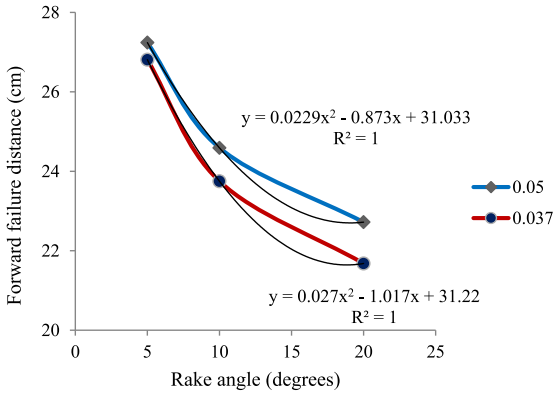

Fig. 14. The relationship between forward failure distance and rake angle.

3.2. *Effect of forward speed and rake angle on the lift height*

The effect of forward speed and rake angle on the lift height is presented in Table 3 and Fig. 12. Table 3 indicates that the change in rake angle was effective on lift height ($P < 0.01$) while the change in the forward speed was not. Also, the interaction effect of forward speed and rake angle on lift height was not significant. The maximum lift height occurred in treatment 5 and at a rake angle of 20°. Moreover, the lift height increased with the increase in the rake angle. Fig. 11 indicates that the relationship between lift height and rake angle was almost linear at 0.05 m/s forward speed, yet it was not linear at 0.037 m/s. Similarly [33], found that the vertical stresses of soil increased with the increase in the working depth and rake angles.

3.3. *Effect of forward speed and rake angle on the failure side area*

Table 3 and Fig. 13 illustrate the response of the failure side area to the changes in the forward speed and rake angle. The Analysis of variance indicated that the change in forward speed was not effective on the failure side area, but the change in the rake angle was effective ($P < 0.01$). Furthermore, the forward speed and rake angle interaction effect were not significant. Maximum failure side area occurred in treatment 5 and at the rake angle of 20°. Moreover, the failure side area increased as the rake angle increased. Fig. 12 indicates that the relationship between failure side area and rake angle was not linear at two forward speeds of 0.037 and 0.05 m/s. The failure side area was not considered in previous studies.

3.4. *Effect of forward speed and rake angle on the forward failure distance*

The response of the forward failure distance to the changes in forward speed and rake angle are shown in Table 3. The results demonstrate that the change in the forward speed was not effective on the forward failure distance, but the change in the rake angle was effective ($P < 0.01$). Moreover, the forward speed and rake angle interaction effects were not significant. Fig. 14 shows that by increasing the rake angle, forward failure distance linearly decreased at both speeds. The ratio of forward failure distance/tine width was calculated against the tine aspect ratio and compared with values obtained by Refs. [7,28,34] where they showed similar trends. The obtained results were similar to that postulated by Ref. [4]. [22] found that forward failure distance increased with the rake angle.

Table 4
Regression models of the studied parameters.

Parameter	Model
Lift height (cm)	7.266–94.615 speed + 0.046 rake angle
Failure side area (cm^2)	208.195–1883.333 speed + 1.306 rake angle
Forward failure distance (cm)	14.61 + 268.974 speed - 0.158 rake angle

Table 5
The different ANFIS models for the lift height.

Item	Type of MFs		Number of MFs		MSE	R^2
	Input	Output	Input	Iteration		
ANFIS 1	Trimf	Linear	3,2	30	0.0545	0.961
ANFIS 2	**Gaussmf**	**Linear**	**3,2**	**30**	**0.0156**	**0.999**
ANFIS 3	Pimf	Linear	3,2	30	0.0866	0.922
ANFIS 4	dsigmf	Linear	3,2	30	0.0302	0.943
ANFIS 5	Tramf	Linear	3,2	30	0.0611	0.957
ANFIS 6	Gbellmf	Linear	3,2	30	0.0401	0.978

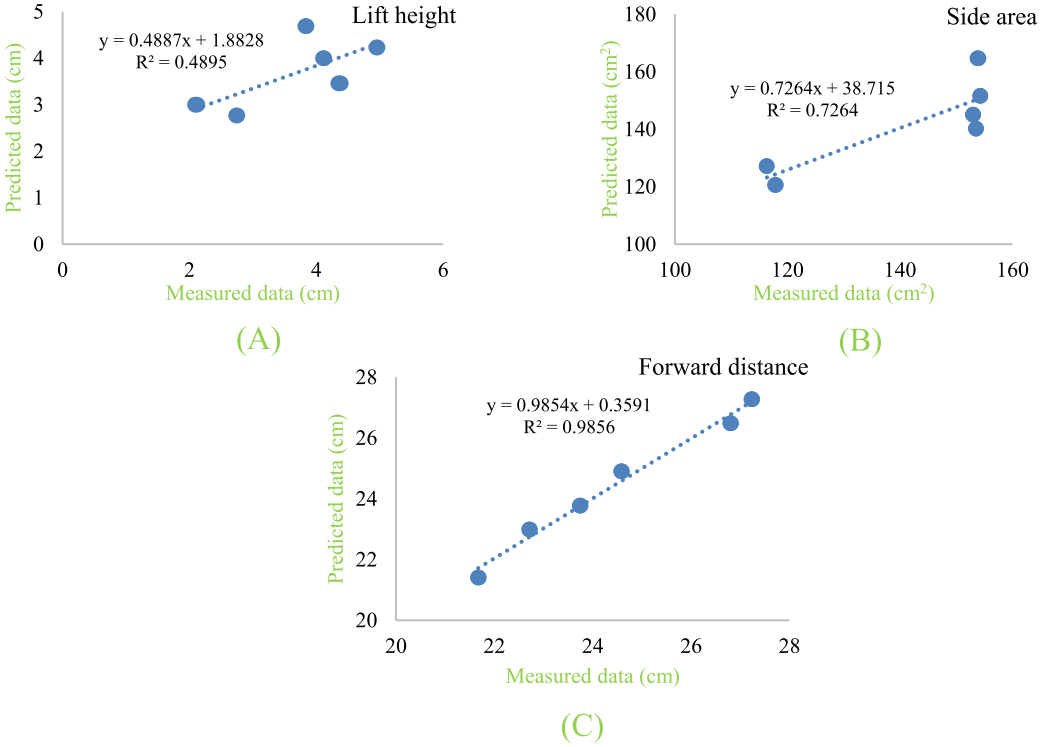

Fig. 15. The correlation between measured and predicted data by linear regression method about (A) lift height (cm), (B) side area (cm^2) and (C) forward distance (cm).

The results of the two researches were different because the tine and soil used for the two exams were different.

Generally, it was found that the adding rake angle caused to increment of lift height and failure side area but decrement of forward failure distance.

3.5. Regression

For each parameter, a separate regression model was developed to predict the lift height, failure side area and forward failure distance of the tested tine using the measured data and SPSS software version 16 (SPSS Inc., IBM, Chicago, IL, USA) which are presented in Table 4 while considering the change of input parameters (forward speed and rake angle). The obtained models were

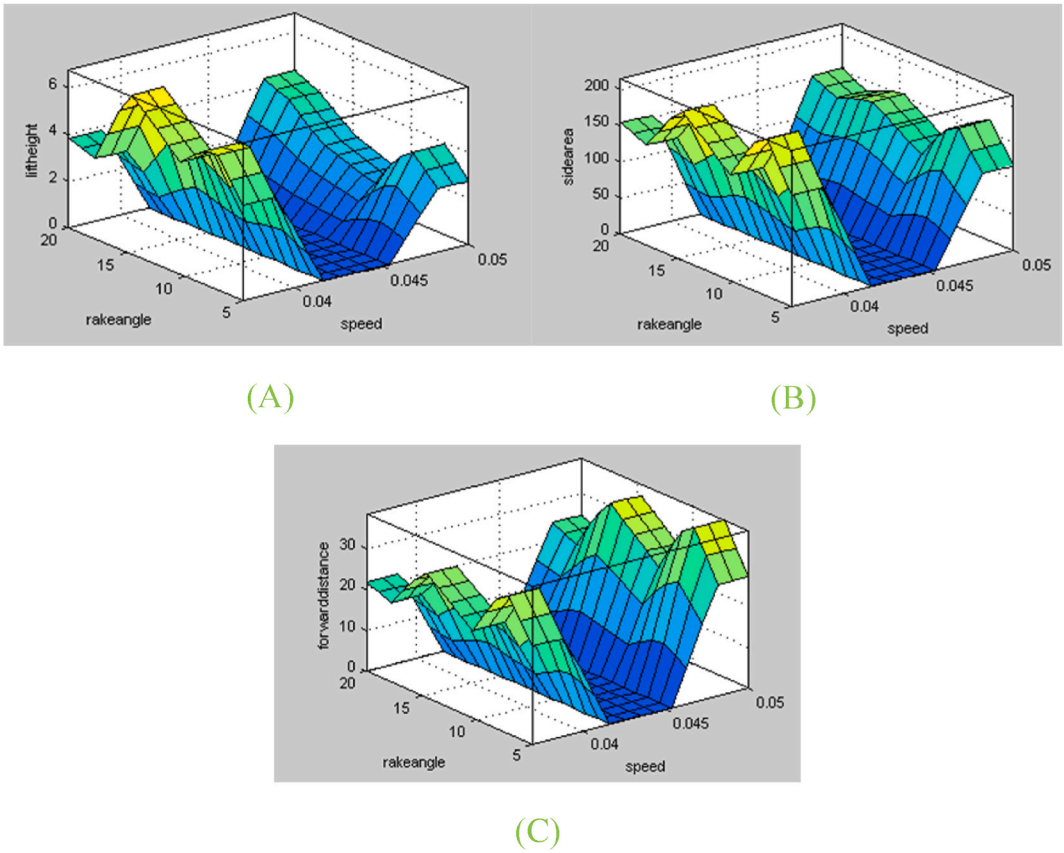

Fig. 16. The output ANFIS diagrams about soil failure; (A) lift height (cm), (B) side area (cm^2) and (C) forward distance (cm).

compared with the data in the preliminary tests to assess their accuracy.

The regression equations were assessed against the obtained data from the tests, as shown in Fig. 15. This figure shows that the existing models predict the studied parameters with different (R^2) accuracy. The lowest and highest accuracy is about lift height and failure forward distance, with the R^2 of 0.4895 and 0.9856.

3.6. ANFIS

Many ANFIS models with various MFs were developed to find the best ANFIS model for lift height, side area and forward distance. For example, the results of Table 5 show that the Gaussian membership function (Gaussmf) configuration was found to denote MSE of 0.0156 and R^2 of 0.9999, consequently it was the best ANFIS model for the lift height. This was done for other two parameters to find best ANFIS models. The distributions of the lift height, side area and forward distance of soil failure caused by studied tine under the effect of forward speed and rake angle using ANFIS are depicted in Fig. 16. This figure can be used to calculate the model's output for specific and non-measured input values. The fitting lines are given as $y = ax + b$ for the lift height, side area and forward distance of soil failure, shown in Fig. 17. Coefficient of determination values of 0.9999, 1 and 1 were obtained for the mentioned failure parameters, respectively. These coefficients are higher than regression ones showing ANFIS is more accurate than the regression. Moreover, these satisfactory results confirm the promising ability of ANFIS-based modelling for prognostication of soil failure characteristics.

4. Conclusions

A soil bin was developed to study the interaction between soil and narrow tines until 5 cm width. Preliminary tests were conducted using a curved chisel tine with two forward speeds and three rake angles to demonstrate the facility's capability. The results indicated that the change in the speed was not effective on the lift height, failure side area and forward failure distance, while the change in the rake angle was effective ($P < 0.01$). Furthermore, the forward speed and rake angle interaction effect was insignificant. Also, with the rise in the rake angle, the lift height and failure side area increased while the forward failure distance decreased. The relationship between the changes in the lift height and rake angle was almost linear at 0.05 m/s forward speed, yet it was not linear at 0.037 m/s. At both speeds, the relationship between the changes in the failure side area and rake angle was not linear. In contrast, the relationship between the changes in the forward failure distance and rake angle was linear. There was similar trend between the soil failure pattern

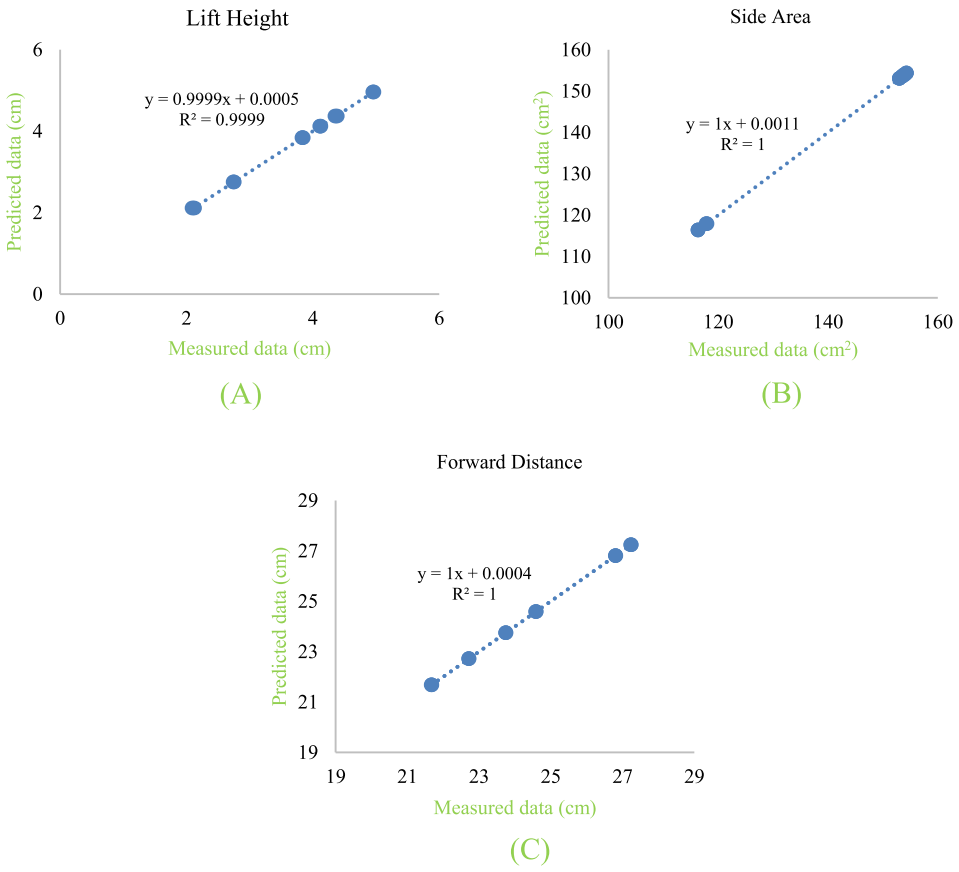

Fig. 17. The correlation between measured and ANFIS predicted data about soil failure; (A) lift height (cm), (B) side area (cm^2) and (C) forward distance (cm).

of the tests and Godwin and Spoor's model. It was confirmed that the new test facility is reliable and more efficient when conducting experiments with narrow tines. Moreover, the linear regression modelling showed that the models predicted the parameters with different accuracy plus the lowest and highest accuracy (R^2 between predicted and measured data) was about lift height and failure forward distance with the R^2 of 0.4895 and 0.9856, relatively. On the other hand, The R^2 of ANFIS models were relatively 0.9999, 1, 1 for lift height, side area and forward distance. Therefore, ANFIS approach was more accurate for predicting soil failure parameters if operating depth does not reach the critical depth.

Data availability statement

No data was used for the research described in the article.

CRediT authorship contribution statement

Arash Lajani: Data curation. **Ali Mohammad Nikbakht:** Project administration. **Mohammad Askari:** Software. **Mahmood Reza Salar:** Validation.

Declaration of competing interest

The authors declare that they have no known competing financial interests or personal relationships that could have appeared to influence the work reported in this paper.

References

[1] O.A. Ani, B.B. Uzoejinwa, A.O. Ezeama, A.P. Onwualu, S.N. Ugwu, C.J. Ohagwu, Overview of soil-machine interaction studies in soil bins, Soil Tillage Res. 175 (2018) 13–27, https://doi.org/10.1016/j.still.2017.08.002.

[2] O. Conte, R. Levien, H. Debiasi, S.L.K. Sturmer, M. Mazurana, J. Muller, Soil disturbance index as an indicator of seed drill efficiency in no-tillage agro-systems, Soil Tillage Res. 114 (2011) 137–142, https://doi.org/10.1016/j.still.2011.03.007.
[3] Y. Chen, L.J. Munkholm, T. Nyord, A discrete element model for soil–sweep interaction in three different soils, Soil Tillage Res. 126 (2013) 34–41, https://doi.org/10.1016/j.still.2012.08.008.
[4] R.J. Godwin, G. Spoor, Soil failure with narrow tines, J. Agric. Eng. Res. 22 (4) (1977) 213–228, https://doi.org/10.1016/0021-8634(77)90044-0.
[5] E. McKyes, O.S. Ali, The cutting of soil by narrow blades, J. Terramechanics 14 (2) (1977) 43–58, https://doi.org/10.1016/0022-4898(77)90001-5.
[6] J.V. Stafford, An application of critical state soil mechanics: the performance of rigid tines, J. Agric. Eng. Res. 26 (5) (1981) 387–401, https://doi.org/10.1016/0021-8634(81)90115-3.
[7] J.V. Perumpral, R.D. Grisso, C.S. Desai, A soil tool model based on limit equilibrium analysis, Trans. ASAE (Am. Soc. Agric. Eng.) 26 (4) (1983) 991–995.
[8] G. Rajaram, D.C. Erbach, Soil failure by shear versus modification by tillage: a review, J. Terramechanics 33 (6) (1996) 265–272.
[9] S. Karmakar, R.L. Kushwaha, Dynamic modeling of soil-tool interaction: an overview from a fluid flow perspective, J. Terramechanics 43 (4) (2006) 411–425.
[10] O. Simon, A. Ovat Friday, O. Okan Orok, Draughts, power requirements and soil disruption of subsoilers, International Journal of Emerging Engineering Research and Technology 6 (9) (2018) 24–38.
[11] J.T. Makanga, V.M. Salokhe, D. Gee-Clough, Deformation and force characteristics caused by inclined tines in loam soil with moisture content below liquid limit, J. Agric. Sci. Technol. 12 (2) (2010) 182–205. http://ir.jkuat.ac.ke/handle/123456789/2339.
[12] U.A. Rosa, D. Wulfsohn, Soil bin monorail for high-speed testing of narrow tillage tools, Biosyst. Eng. 99 (3) (2008) 444–454, https://doi.org/10.1016/j.biosystemseng.2007.11.010.
[13] K.A. Aikins, T.A. Jensen, D.L. Antille, J.b. Barr, M. Ucgul, J.M.A. Desbiolles, Evaluation of bentleg and straight narrow point openers in cohesive soil, Soil Tillage Res. 211 (2021) 105004.
[14] A.K.A. Al-Neama, Evaluation of Performance of Selected Tillage Tines Regarding Quality of Work, Springer Berlin Heidelberg, 2019, https://doi.org/10.1007/978-3-662-57744-8.
[15] E. Volpe, S.L. Gariano, F. Ardizzone, F. Fiorucci, D. Salciarini, A heuristic method to evaluate the effect of soil tillage on slope stability: a pilot case in central Italy, Land 11 (6) (2022) 912, https://doi.org/10.3390/land11060912.
[16] L.V. Fechete-Tutunaru, F. Gaspar, Z. Gyorgy, Soil-tool interaction of a simple tillage tool in sand, E3S Web Conf 85 (2019) 08007, https://doi.org/10.1051/e3sconf/20198508007.
[17] S.I. Manuwa, A.A. Ajisafe, Development of overhead gantry as complementary equipment to indoor soil bin facility, J. Food Technol. 8 (3) (2010) 92–95, https://doi.org/10.3923/rjasci.2010.92.95.
[18] A.S. Adesanya, Electrically-controlled System for Overhead Gantry Trolley for Indoor Soil Bin Operations Meng Thesis, Department of Agricultural Engineering Federal University of Technology, Akure, Nigeria., Akure, 2012. http://196.220.128.81:8080/xmlui/handle/123456789/3504.
[19] R. Hegazy, M. Okasha, Design and Use Open Air Soil Bin for Testing Farm Machinery' Components, Academic Catalog. Agricultural Engineering Department, Faculty of Agriculture, Kafrelsheikh University, Egypt, 2020, https://doi.org/10.13140/RG.2.2.11375.05284/1.
[20] M. Yousefi, S.R. Mousavi Seyedi, M. Askari, Predicting the soil-Wheel contact area under the effect of vertical load, tire inflation pressure and forward speed at soil bin using ANFIS, Agricultural Mechanization and system research 22 (80) (2022) 67–76.
[21] Q. Zhang, Y. Lin, Analysis of failure mode of reinforced embankments overlying voids based on discrete method, Appl. Sci. 13 (16) (2023) 9270, https://doi.org/10.3390/app13169270.
[22] O.B. Aluko, H.W. Chandler, Characterisation and modeling of brittle fracture in two-dimensional soil cutting, Biosyst. Eng. 88 (3) (2004) 369–381, https://doi.org/10.1016/j.biosystemseng.2004.03.009.
[23] S.M. Shafaei, M. Loghavi, S. Kamgar, Appraisal of Takagi-Sugeno-Kang type of adaptive neuro-fuzzy inference system for draft force prediction of chisel plow implement, Comput. Electron. Agric. 14 (2) (2017) 406–415, https://doi.org/10.1016/j.compag.2017.09.023.
[24] S.M. Shafaei, M. Loghavi, S. Kamgar, M.H. Raoufat, Potential assessment of neuro-fuzzy strategy in prognostication of draft parameters of primary tillage implement, Annals of Agrarian Science 16 (3) (2018) 257–266, https://doi.org/10.1016/j.aasci.2018.04.001.
[25] M. Askari, Y. Abbaspour-Gilandeh, Assessment of adaptive neuro-fuzzy inference system and response surface methodology approaches in draft force prediction of subsoiling tines, Soil Tillage Res. 194 (2019) 104338, https://doi.org/10.1016/j.still.2019.104338.
[26] A.P. Onwualu, Tillage Tool Factors Affecting Sandy Soil Interaction with Plane Blades in a Bin, PhD Thesis, Technical University of Nova Scotia, Halifax, Canada, 1991.
[27] ASABE Standards, Agricultural machinery management data, ASAE D497 (2011) 7. R2020, https://elibrary.asabe.org/abstract.asp?aid=36431.
[28] X. Jiang, J. Tong, Y. Ma, J. Sun, Development and verification of a mathematical model for the specific resistance of a curved subsoiler, Biosyst. Eng. 190 (2020) 107–119.
[29] I. Shmulevich, State of the art modelling of soil-tillage interaction using discrete element method, Soil Tillage Res. 111 (1) (2010) 41–53.
[30] S.R. Ashrafizadeh, R.L. Kushwaha, Soil failure model in front of a tillage tool action. A Review. Presentation at the CSAE/SCGR Meeting, Canada, Montreal, Quebec, 2003. July 6–9.
[31] H.K. Celik, N. Caglayan, M. Topakci, A.E.W. Rennie, I. Akinci, Strength-based design analysis of a Para-Plow tillage tool, Comput. Electron. Agric. 169 (2020) 105168.
[32] S. Rahman, Y. Chen, Laboratory investigation of cutting forces and soil disturbance resulting from different manure incorporation tools in a loamy sand soil, Soil Tillage Res. 58 (1) (2001) 19–29, https://doi.org/10.1016/S0167-1987(00)00181-1.
[33] Ch Hang, Y. Yao, Y. Huang, W. Li, R. Zhu, High-speed photographic analysis of the soil disturbance affected by subsoiler rake angle, Agricultural Engineering International: CIGR Journal 19 (2) (2017) 42–50.
[34] J. Ndisya, A. Njoroge Gitau, D.O. Mbuge, A.W. Hiuhu, Investigation of the effect of rake angle on draft requirement for ripping in sandy clay, Agricultural Engineering International: CIGR Journal 18 (4) (2016) 52–69.